Rheologica Acta manuscript No.
(will be inserted by the editor)

Rheology of cave sediments: application to vermiculation

Perrine Freydier[1], Jérôme Martin[1], Béatrice Guerrier[1], Pierre-Yves Jeannin[2], Frédéric Doumenc[1,3]

[1] Laboratoire FAST, Université Paris-Sud, CNRS, Université Paris-Saclay, F-91405, Orsay, France
[2] Swiss Institute for Speleology and Karstology (SISKA), La Chaux-de-Fonds, CH-2301, Switzerland
[3] Sorbonne Université, UFR 919, 4 place Jussieu, F-75252, Paris Cedex 05, France

Received: date / Revised version: date

Abstract Several cases of vermiculations formation have been reported in painted caves, with potential issues for the conservation of parietal prehistoric paintings. Vermiculations are natural patterns observed in caves. They result from displacement of sediment initially at rest on cave walls. The collapse of the sediment yield stress, which allows the sediment to flow under small mechanical stresses could be a necessary first step of the vermiculation process. Two possible scenarios have been identified: (1) when the sediment is soaked in low-mineralized water, a rapid and limited drop of the yield stress is followed by a slow decrease, which can seriously weaken the sediment layer if soaking is continued over several months and (2) a spectacular decrease of the yield stress (two orders of magnitude) when the sediment is soaked within a solution enriched in monovalent cations for weeks and suddenly exposed to low-mineralized water. The specific behaviour of smectite clays binding the sediment accounts for this loss of cohesion.

1 Introduction

Vermiculations are specific patterns of sediments observed on cave walls (Fig.1a). As defined by A. Bini and co-workers, "vermiculations are thin, irregular and discontinuous deposits of incoherent materials commonly found on the walls of caves and external surfaces and are a few centimetres in extents". The thickness of vermiculations ranges from less than 1 millimetre up to 10 millimetres [Bini et al., 1978]. Although this natural phenomenon has been observed and studied for a very long time (E.-A. Martel mentions "thin ribbons of clay" in a cave of the valley of Verdon (France) in 1906 [Martel, 1906]), the physical mechanisms that produce these patterns are still to be elucidated.

Beyond the scientific curiosity, addressing this issue is of high importance for the conservation of parietal prehistoric paintings, potentially damaged by the vermiculation process [Konik et al., 2014]. Vermiculations arised in Niaux cave (Arrière, France) in 1978 and 1979 ([Clottes, 1981] and Fig.1b), and in Lascaux cave (Dordogne, France) in 2009 [Hœrlé et al., 2011]. The present study was commissioned by the Scientific Council of Lascaux cave as part of its study program "Vermiculations in Lascaux cave". The monitoring of painted caves showed that vermiculations grow during periods of crisis, with a characteristic time of formation of the order of weeks, possibly shorter (in any case, a tiny time compared with the age of paintings, estimated to 18,000 years in Lascaux).

Most of the state of knowledge on vermiculations in caves can be found in the review by A. Bini and coworkers [Bini et al., 1978], and in two more recent documents: [Hœrlé et al., 2011] and a technical report (not published) dedicated to the Lascaux cave [Hoerlé, 2012]. The literature on vermiculations mainly reports descriptive studies based on field observations. Vermiculations have been observed on many substrates in caves, in most cases on limestone, but also on concrete, mud, rubber of electric cables [Bini et al., 1978]. Vermiculations contain a wide variety of materials: particles of mineral matter (quartz, calcite, metallic oxydes, aluminosilicates including clays...) and organic matter (including a large variety of living microorganisms such as mushrooms, algae, bacteria...) [Hoerlé, 2012]. Analysing the vermiculations of Lascaux cave, S. Hoerlé and co-workers point out the similarity between the materials found inside the vermiculations and those present nearby on the wall. The authors suggest that "fine, easily mobilized particles, present on the cave walls (dust, rock alteration products, deposits, pigments, bacteria...) migrate on few centimetres or metres along the wall and form vermiculations" [Hœrlé et al., 2011].

It is generally admitted that the presence of water is required to get vermiculations [Barr, 1957, Bini, 1975]. Water can lead to mobilization and displacement of particles, followed by particles aggregation and pattern for-

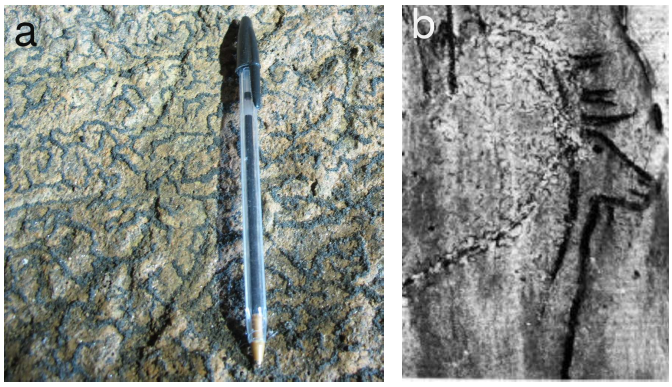

Fig. 1 Examples of vermiculations. a) Wall of Maillol cave. b) Degradation of wall paintings in the cave of Niaux (credit: J. Clottes, first published in ref. [Clottes, 1981]).

mation. In the case of Niaux cave, vermiculations occured after a sudden water intake, and the solution to preserve paintings was to divert the major part of the runoff away from the paintings. However, the presence of water is not a sufficient condition. Indeed, a seasonal thin film of water, which may originate from percolation or condensation, has been observed every year on the walls of the Hall of Bulls in Lascaux cave, while a single vermiculation crisis has been reported, between 2009 and 2010.

Vermiculations are mainly observed in areas with a significant air exchange with the outside atmosphere (close to caves entrance, or in narrow sections) [Bini et al., 1978], or in shallow caves (lower than 10 m depth) as in the Wilson cave [Faucher and Lauriol, 2016]. Therefore, in most cases vermiculations are observed where yearly temperature variations can generate significant temperature gradients. These observations suggest a possible role of condensation and evaporation in the vermiculation process.

Many hypotheses have been suggested to explain vermiculations. After presenting a review, [Bini et al., 1978] proposed "a unitary theory of vermiculation genesis", which is one of the most popular theory up to now. These authors assume that all the fine-grains materials susceptible to form vermiculations are initially suspended in the water film lying on cave walls. Evaporation or any change in the physicochemical conditions (pH, temperature...) trigger a loss of colloidal stability and particles agglomerate, forming patterns. An interesting aspect of Bini's theory is the major role played by colloidal interactions. However, it is a qualitative approach, which does not explain the migration of sediments initially at rest on cave walls.

The present work addresses the first step of the vermiculation issue, by investigating conditions leading to a loss of cohesion of the sediment lying on cave walls. It is a well documented fact that the granulometry of cave sediments is characterized by a wide particle size distribution, including a significant amount of colloidal particles [Ford and Williams, 2007]. Moreover, it has been widely shown that such wet materials can exhibit a yield stress [Coussot and Ancey, 1999] (the yield stress is the stress threshold above which the material flows as a viscous fluid and below which it behaves as a solid).

We hypothesize that particle migration along the wall requires the sediment yield stress to be overcome by any external force, caused for instance by gravity, water film flow, Marangoni effect... Accordingly, two scenarios may occur: (1) an increase of an external force (e.g. in presence of a water film flow, a rise of the flow rate induces an increase of the viscous stress on the sediment) and (2) a decrease of the sediment yield stress, triggered by a modification of some physicochemical factors in the cave environment. In the present work, we investigate the latter point. For instance, a 1 mm thick sediment deposit on a vertical wall can be displaced by gravity if the yield stress sediment decreases below the gravity shear stress $\rho g h \sim 10\,\mathrm{Pa}$ (where ρ is the sediment density, g the gravitational acceleration and h the thickness of the sediment layer). In laboratory experiments, we measured the yield stress evolution of a cave sediment in a range of conditions potentially found in a cave environment, in order to identify conditions leading to a significant decrease of the yield stress.

We selected for these laboratory experiments a natural sediment collected in a cave in which vermiculations are present. The cohesion of the sediment is expected to result from colloidal matter binding all particles of the sediment together. Thence, colloidal interactions must be taken into consideration to improve our understanding of sediment cohesion (see for instance [Anger, 2011] for a complete review of colloidal matter in soils). X-ray diffraction analysis revealed that the main colloidal matter in our selected material was smectite clay.

Smectite is composed of thin aluminosilicate platelets (typically 1 nm thick and $50 - 500\,\mathrm{nm}$ lateral dimensions), with permanent negative charges on their faces, balanced by exchangeable counterions. Its swelling capacity and mechanical properties result from a balance between repulsive and attractive forces between particles. Repulsion arises from osmotic pressure induced by the interpenetration of counterion diffuse layers. Hence, increasing the solution ionic strength reduces the diffuse layer length, allows particles to get closer to each other [Larson, 1999] and results in a lower repulsion force. Attractive forces are twofolds: van der Waals interactions, which are short range forces and which are negligible for the low ionic strengths - much lower than 1 M - considered in the present work [Norrish, 1954, Jönsson et al., 2009], and ion-ion correlation forces, which increase with the particle surface specific charge and the counterion valence [Segad et al., 2010]. Moreover, variable charges are also present at platelet edges, so one must also consider edge-to-face electrostatic interactions [Martin et al., 2002, Hedström et al., 2016], which can either be attractive or repulsive, when edge

variable charges are respectively positive (at low pH), or negative (at high pH). The literature provides very scattered data for the isoelectric point of platelet edges (values ranging from pH 4 to 11 have been proposed, see [Hedström et al., 2016] for a review). In positive edge charge conditions, attractive edge-to-face interactions can lead to gel formation.

Because of the colloidal matter (mainly smectite in our case) contained in the sediment, we expect the pH, the ionic strength, and the nature of the ions present in the water to have significant effects on its cohesion. In caves, sediments are in contact with percolated water of high mineral content and varying compositions, or with condensation water. In addition, variations of the CO_2 partial pressure (pCO_2) in the atmosphere can modify the water pH because of carbonic acid formation due to CO_2 dissolution. These situations are reproduced in our experiments by soaking sediment samples in solutions of controlled compositions, under an atmosphere of controlled pCO_2. The time evolution of the sediment cohesion is monitored by varying the soaking time before batch measurement of the yield stress in a rheometer. We first investigate the effect of a single soaking in a saline solution with various salts (which mimics percolated water of various compositions) or in deionized (DI) water (which mimics condensation water). We then investigate the case of two consecutive soakings, the first in saline water and the second in DI water (in a cave environment, this would correspond to a percolated water intake followed by a condensation event).

The remaining part of the paper is organized in 3 sections. In section 2, we present the characterization of the cave sediment used in the experiments, along with the experimental set-up. Results of soaking experiments are presented for a wide range of cave conditions and discussed in section 3. Conclusions are drawn in Section 4.

2 Material and methods

2.1 Mineralogical characterization and granulometry of the sediment

The investigated cave sediments have been collected in 2016 and 2017 in Maillol natural cave in Dordogne, France (GPS coordinates: 45.042°N, 1.168°E). As most caves in the world, Maillol cave is located in a karst massif. Karst formation is a process leading to specific landforms (e.g. caves) and hydrology (rainfall is mainly routed underground). Karst results from the dissolution of the bedrock, usually limestone, which is composed of calcium carbonate ($CaCO_3$), and is soluble in rainfall water. The cave is situated rather shallow (0 - 9 m below ground), and presents vermiculations over most of its walls (Fig.1a). The sediment has been collected on the floor of the cave directly below a vermiculated wall, at about 30 m from the entrance. When collected, the sediment was in a state of cohesive and compact paste.

The Maillol cave sediment was characterized according to the following aspects: mineralogical composition, titration of calcium carbonate, granulometry, cation-exchange capacity (CEC) and organic matter quantification. All these characterisations have been done by GEOPS laboratory (UMR 8148, Paris-Sud University, CNRS). X-ray diffraction revealed the presence of high quantities of quartz and calcite, and lower amounts of many other minerals like metallic oxydes and hydroxydes, igneous minerals and various phyllosilicates (clay-minerals). X-ray diffraction of the sediment fine fraction ($\leq 2\mu$m) was applied following the three usual protocols for clays: (1) on the original sample, (2) after treatment with ethylene-glycol and (3) after heating at 550°C. Smectite appears to be the dominant clay-mineral (80% of the fine fraction). Other detected clays are kaolinite, illite and chlorite, approximately in the same proportions.

Sediments granulometry has been measured with a laser granulometer (Malvern Mastersize 2000). Fig. 2 displays the corresponding particle size distribution. The presence of coarse grains in the raw sediment is incompatible with the use of a rheometer. We thus removed all particles with a diameter above about 200 μm. For this purpose, the sediment has been slightly dried for 48 h at ambient air (final solid mass fraction was about 95%). Then the aggregates have been gently crushed with a mortar, and all particles with a diameter above 200 μm (4% volume fraction) have been removed with a dry sieving. We checked that, after crushing and sieving, granulometry of particles smaller than 200 μm was almost unchanged (see Fig. 2). The D_{10}, D_{50}, and D_{90} of the sieved sediment are 6.2 μm, 47 μm and 136 μm respectively (D_{10}, D_{50}, and D_{90} are the grain diameters corresponding to 10, 50 and 90% of particle volume smaller than a certain size). With such an amount of fine particles (more than 10% of particles under 10 μm), the sediment is expected to be cohesive and to exhibit a yield stress [Coussot and Ancey, 1999]. The small amount of removed large particles ($\geq 200\,\mu$m) is not expected to modify the global rheological behaviour [Ovarlez et al., 2015].

The mass fraction of calcium carbonate in the sediment is about 20%, obtained by soaking the sediment in DI water, then measuring by atomic absorption the calcium concentration of the resulting solution (under-saturated with respect to $CaCO_3$). Organic matter mass fraction is about 3%, obtained by measuring the weight loss after 2 h 30 min at 550°C in an oven. Sediment average density, measured with a pycnometer, is 2630 $kg.m^{-3}$, in line with the nature of the sediment components. The CEC of the material is 20 $cmol+.kg^{-1}$. It has been measured according to the method of [Aran et al., 2008] and represents the ability

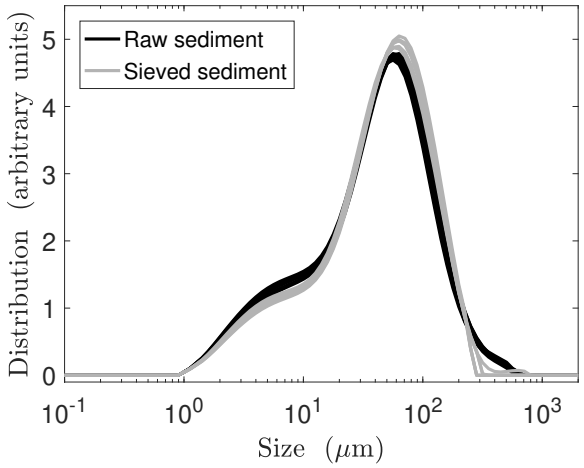

Fig. 2 Volume particle size distribution of the raw sediment and the sieved sediment (in either case, six measurements of the same sample are superimposed).

of the material to exchange cations with the surrounding aqueous solution.

Several other sediments and vermiculations were also collected in other (painted and not painted) caves in Dordogne (France), including Lascaux, in order to assess the variability of their characteristics. Results from X-ray diffraction and granulometry were very similar. The Maillol cave sediment used in the present work can therefore be considered as a model material for the study of the vermiculations in Lascaux cave, and incidentally in other caves in Dordogne.

2.2 Rheological characterization of the sediment

2.2.1 Protocol for rheological characterization. Samples with different solid mass fractions were prepared by adding DI water (electrical resistivity: 18 MΩ.cm) to the material and mixing it manually with a spatula. The solid mass fraction, denoted W_s, is expressed as the ratio of the dry mass to the total mass (the water mass fraction is thus $1 - W_s$). The total and dry masses are measured by weighing a small sample before and after a 24 hours drying in a vacuum oven at 105°C.

Rheometrical measurements were performed using an Anton Paar Physica MCR 501 rheometer equiped with a 25 mm parallel-plate geometry. Plates with 100 μm roughness (ref. INSET I-PP80/SS, Anton Paar) were used to avoid sample slip during the test. Sample temperature was kept constant at 20°C. We used a protective dome to prevent evaporation of water from the sample.

The gap between the two plates of the rheometer was varied between 500 μm and 1500 μm. No variation in the measured yield stress was observed. We then fixed the gap at 500 μm for all tests. To cope with clay material thixotropy and obtain reproducible results, a pre-shear ($50\,s^{-1}$ during 20 s) followed by a rest time (10 s) was applied before each measurement. We checked that moderate variations of these parameters did not significantly affect the results.

To measure the yield stress τ_c, we recorded the shear rate as a function of time for an imposed stress [Magnin and Piau, 1987, Coussot et al., 2002, Khaldoun et al., 2009] (the measurement time and the sampling rate have been set to 120 s and 0.5 Hz, respectively). Typical curves are displayed in Fig. 3a for $W_s = 57.7\%$ and 3c for $W_s = 66.0\%$. At low imposed stress, the shear rate decreases with time and tends continuously to zero, meaning that the sample is in a solid state. At high imposed stress, the shear rate reaches a constant value after a short transient, meaning that the sample behaves like a fluid, with a finite viscosity. The yield stress is the critical stress at which a solid-fluid transition is observed, characterized by a drastic change in shear rate when the imposed stress is increased (in practice, the yield stress is defined as the smallest value of the stress for which we surely observe a fluid behaviour). For instance, on Fig. 3a, the shear rate after 120 s increases by 5 orders of magnitude when the imposed stress increases from 135 to 140 Pa, which only represents a 4% relative variation of the stress. This indicates a sudden liquefaction of the material. Such an abrupt transition, which made the determination of the yield stress unambiguous, was observed for most tested samples. The transition was however less clear for a few samples corresponding to very low yield stress ($\tau_c < 10$ Pa). For these samples, only a higher bound of τ_c could be determined.

Before each determination of the yield stress τ_c, a small amount of sediment was systematically collected from the sample and used to measure the corresponding solid mass fraction W_s. Good adhesion of the sample to the plates was checked after each test by visual inspection (presence of a cone or fingering in the plate-plate geometry after removal of the upper plate, see Fig. 3b,d [Magnin and Piau, 1987, Magnin and Piau, 1990]). We measured yield stress up to 6000 Pa without sliding or fracturing. The reproducibility of the measured yield stress was ±18% (twice the standard deviation of ten different measurements on identical samples).

2.2.2 Effect of water content on the sediment yield stress. Fig. 4 displays the yield stress measured for different solid mass fractions (black symbols). For solid mass fractions varying from 47.4% to 68% (corresponding to solid volume fractions from 25.5% to 44.6%) we obtained yield stresses ranging from 14 to 6000 Pa (maximum measurable stress in our conditions). All measurements fit pretty well with the following relationship:

$$\tau_c = 1.6 \times 10^{-6} \exp(32.6\, W_s). \quad (1)$$

This kind of relation is common for materials containing clay [Carrière et al., 2018]. Considering the high com-

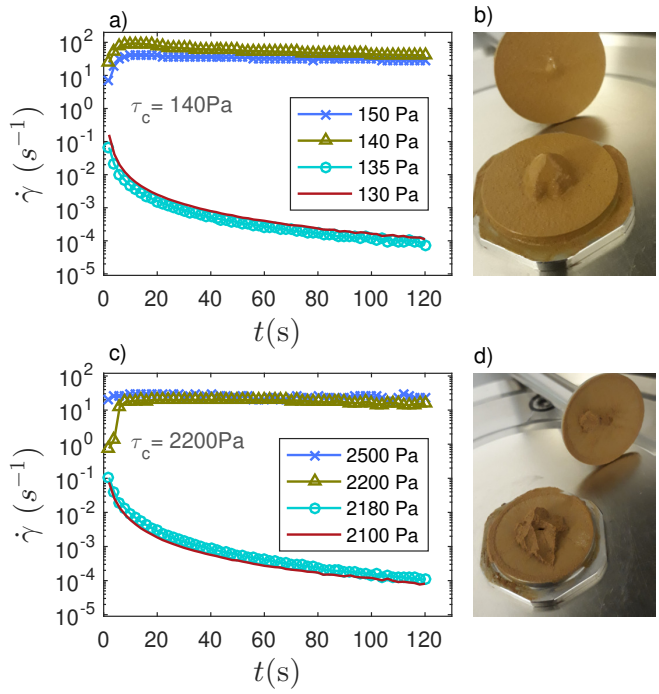

Fig. 3 Determination of the sediment yield stress. Shear rate as a function of time for different imposed stresses (see legend) for $W_s = 57.7\%$ (a) and $W_s = 66.0\%$ (c). Deposit shape after rheological measurement and upper plate removal for $W_s = 57.7\%$ (b) and $W_s = 66.0\%$ (d).

plexity of the natural material under investigation, the merging of the data is very satisfactory. Eq.1 reflects the fact that the yield stress strongly depends on the water content (yield stress variation by more than three orders of magnitude for a 20% variation of water content).

2.3 Soaking experimental set-up

2.3.1 Cave environment. The chemical composition of the water seeping as thin film on a cave wall is poorly known, mainly due to the difficulty to sample a sufficient amount of water for a chemical analysis. If direct measurements are very difficult, one can indirectly assess it by considering the three potential origins of the water. 1) Water may be issued from seepage through fissures and porosity of the rock matrix, and the composition of this type of water is well studied within the frame of paleoclimatological reconstructions from speleothemes (mainly stalagmites). 2) Water on a cave wall may result from a quick and concentrated infiltration of water flooding a cave passage during high water conditions. The composition of this type of water is also well known from the significant litterature concerning karst hydrogeology, more specifically spring chemograph analyses. Waters from both origins are quite similar with a mineralisation dominated by calcium and bicarbonates [Ford and Williams, 2007]. 3) Water can be produced at cave wall by condensation; an important point is that condensation provides initially pure – non-mineralized – water, then its mineralization increases until equilibrium with the solid and gas phases is reached.

Among other factors, $CaCO_3$ solubility in water depends on pCO_2, which governs the concentration of carbonic acid in the liquid phase [Plummer and Wigley, 1976]. Typical pCO_2 values in a cave environment range from 0.04% (4×10^{-4} atm), to 10% (0.1 atm). Corresponding theoretical solubilities of $CaCO_3$ in pure water are 0.5 mM and 3.4 mM, respectively. Note however that $CaCO_3$ solubility in real environments can be increased by acids other than carbonic acid [Gaillardet et al., 2018], or because of calcium complexation by dissolved organic matter as, for instance, humic acids [Reddy et al., 1990]. Cations other than Ca^{2+} are present in karst aquifers, with lower concentrations (Mg^{2+}, Na^{+}, K^{+},...). Most widespread anions are bicarbonate HCO_3^- and carbonate CO_3^{2-} (coming from the dissolution of $CaCO_3$ and atmospheric CO_2), and also Cl^-, NO_3^-, SO_4^{2-} [White, 2015]. All these ions are expected to be present in thin water films lying on cave walls, although their concentration might significantly differ from that of karst aquifers, because (1) some chemical species which are very diluted in karst aquifers may be concentrated in thin liquid films due to seasonal evaporation cycles and (2) microbiological activity could significantly change chemical equilibrium in the liquid film [Barton and Northup, 2007].

2.3.2 Experimental set-up for soaking experiments. Our experiment consists in measuring the evolution of the sediment yield stress for sample deposits soaked in various solutions with compositions covering those encountered in a cave environment. The gas phase is saturated with water vapor to avoid sediment drying, and the pCO_2 is fixed to control the $CaCO_3$ dissolution. The experimental set-up is displayed in Fig. 5. Air and CO_2 are mixed together in desired proportions using two flow-controllers (Brooks Instruments SLA5850), with a flow rate control accuracy better than 0.9%. The resulting blend is saturated with water vapor by bubbling in a water bath. The pCO_2 of the gas injected in the box is recorded for the entire duration of the experiment with a BlueSens BCP-CO_2 sensor (4% accuracy). The gas flow rate is fixed to renew the atmosphere inside the box every 2 minutes. As temperature is not expected to play a significant role, all the experiments are performed at room temperature.

Before each soaking experiment, the material is prepared by mixing sieved sediment and DI water, following the protocol described in section 2.2.1. The initial state of the material is then characterized by measuring the yield stress τ_c and the solid mass fraction W_s. For all the soaking experiments, the initial solid mass fraction has been varied from 58% to 67.5%, corresponding to initial yield stress ranging from 180 to 5000 Pa. A micro-

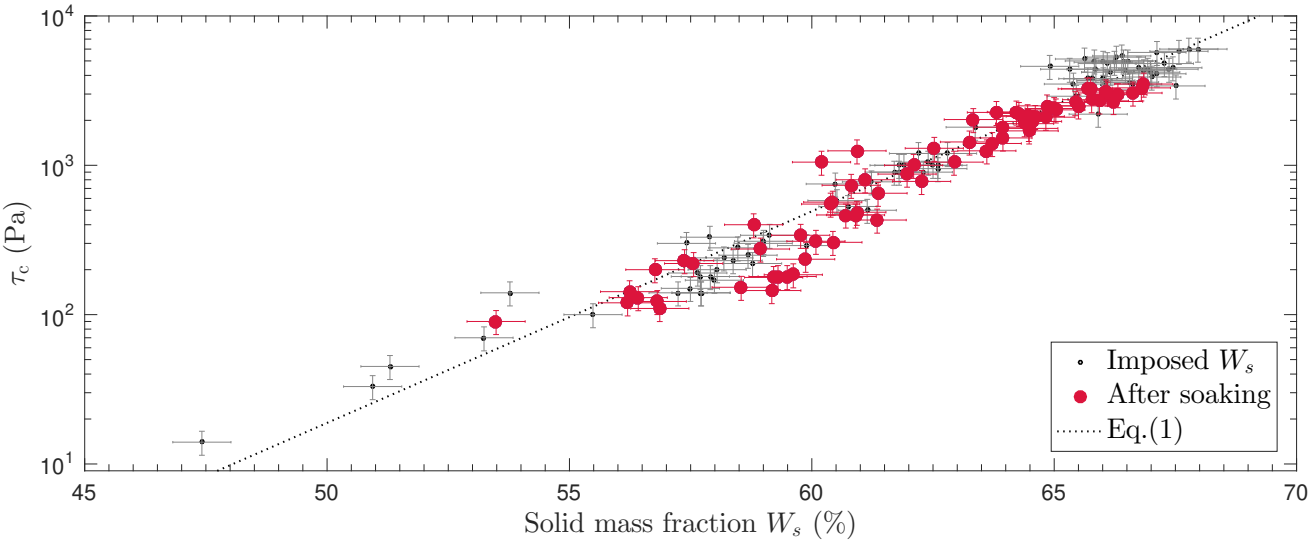

Fig. 4 Yield stress τ_c of cave sediment as a function of the solid mass fraction W_s. Black dots represent all the data obtained by adding a prescribed quantity of water to the sediment (imposed W_s). Red circles display all the values obtained after a single soaking experiment, with no distinction of experimental conditions ; samples were soaked for 20 min to 60 days in one of the following liquids: DI water or $CaCO_3$ saturated solutions at pCO_2 varying from 0.035% to 10%, NaCl (27 mM), KCl (27 mM), $CaCl_2$ (18 or 27 mM) or $MgCl_2$ (27 mM) aqueous solutions at pCO_2 = 0.035% ; the initial solid mass fraction for soaking experiments ranged from 58% to 67.5 % (solution volume: 20 cm^3 in all cases).

scope glass slide is then coated with a 1 mm thick layer of material (sample volume: 2 cm^3). This sample is immediately soaked in a volume of solution fixed at 20 cm^3. The reservoir containing the sample and the soaking solution is then placed in the controlled atmosphere box.

Different compositions of soaking solution have been investigated: DI water or $CaCO_3$ saturated solution under pCO_2 from 0.035% to 10%, solutions of NaCl, KCl, $CaCl_2$ or $MgCl_2$ at pCO_2 = 0.035%. Before receiving the sample, the soaking solution was first equilibrated with the atmosphere at the desired pCO_2 by bubbling (strictly speaking, DI water used for soaking is not fully deionized, since it contains a certain amount of dissolved CO_2). During soaking, the composition of the solution is not expected to remain constant, because of dissolution of minerals included in the sediment (for instance $CaCO_3$, which represents about 20% of the sediment mass, see subsection 2.1). Such dissolution process is also expected in natural environment.

Once the sample is soaked in a solution of a given composition, the exchange of water and ions with the solution is expected to modify the sample yield stress. The soaking time was varied from 20 min to 60 days. At the end of the prescribed soaking time, the solution is removed, the excess of liquid on the glass slide is carefully drained by slightly tilting the slide, and the material is removed from the slide to perform the yield stress and solid mass fraction measurements. The available material on one glass slide allows two or three measurements of the yield stress for reproducibility control.

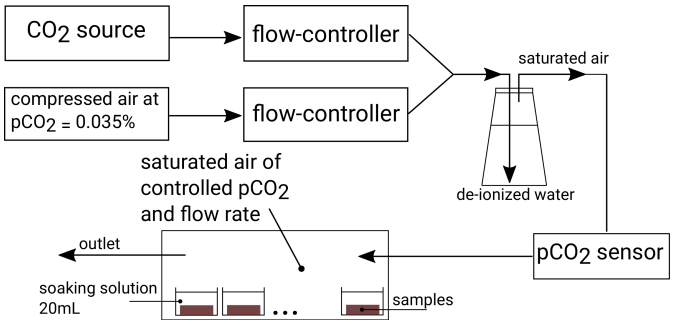

Fig. 5 Soaking experimental set-up.

3 Results and discussion

3.1 Effect of the mineralization of the soaking solution

Fig. 6a displays the time evolution of the yield stress τ_c for samples soaked into DI water or solutions with different concentrations of calcium salts (carbonate or chlorure, the latter allowing higher concentration due to its large solubility in water). The corresponding time evolution of the solid mass fraction W_s (measured on the same sample as τ_c) is presented in Fig. 6b.

For DI water, we clearly observe a fast and large decrease of the yield stress during the first few hours at the beginning of the experiment, followed by a much slower response (black curve, Fig. 6a). The yield stress is divided by about 2.6 after 3 hours of soaking, and by 17 after 25 days. A similar behaviour is observed with calcium carbonate saturated solutions, but with a lower decrease of the yield stress, especially for the highest pCO_2, corresponding to higher $CaCO_3$ concentration (green curve,

Soaking solution	W_s (%)			τ_c (Pa)		
	Initial	Final	ΔW_s	Initial	Final	ratio
DI water	67.5	53.5	-14.0	3400	90	38
$CaCO_3$ sat.	67.5	56.2	-11.3	3400	120	28

Table 1 Sample solid mass fraction (W_s) and yield stress (τ_c) before and after 60 days of soaking in DI water or $CaCO_3$ saturated solution (pCO_2=0.035%).

Fig. 6a). With the high concentration of calcium chloride ($CaCl_2$), only the slow decrease is observed (the yield stress is only divided by 2.3 after 25 days of soaking). The same qualitative behaviours are observed for the time evolution of the solid mass fraction (Fig. 6b), indicating a strong correlation with the yield stress. For a given time, the swelling and the decrease of the yield stress are less pronounced when the mineralization of the soaking solution is higher. This fits well with the reduction of repulsive colloidal forces when the ionic strength of the solution is increased.

Two complementary experiments have been carried out with soaking time increased to 60 days and low-mineralized water: DI water and $CaCO_3$ saturated solution, at pCO_2=0.035% in both cases. Results are presented in table 1. The initial and final yield stresses are of the order of 3000 and 100 Pa respectively. The yield stress was thus divided by about 30 after a 60 days soaking, instead of 17 after 25 days. Such long swelling times (weeks or months), likely due to slow structural reordering, are very common in clay materials [Martin et al., 2006]. A long – several months – exposure to low-mineralized water seriously weakens the sediment cohesion. According to these experimental results, a long soaking in low-mineralized water caused by a long condensation period is a favourable condition for particle migration on a cave wall. Consequently, this is a dangerous situation for caves paintings.

3.2 Effect of cations valency on the cohesion of caves sediment

3.2.1 Single soaking. The final yield stress after a single soaking is plotted in Fig. 4 (red circles) as a function of the final solid mass fraction, for all the experiments performed with various soaking times (20 min to 60 days) and initial solid mass fractions (58% to 67.5%). We used DI water and salt solutions, including salts of a monovalent cation (NaCl, KCl) or a divalent cation ($CaCO_3$, $CaCl_2$, $MgCl_2$), with the aim to change ion-ion correlation forces between colloidal particles (see the caption of Fig. 4 for salt concentrations and pCO_2). In Fig. 4, we deliberately made no distinction between soaking conditions (a more detailed analysis follows). All the soaking experiments align along the master curve (Eq.1) whatever the experimental conditions. The relation between the yield stress and the solid mass fraction remains the same when the sediment is simply mixed with an imposed amount of DI water (black points in Fig. 4) or swelled by soaking in aqueous solution. The key point of these experimental results is that the sediment yield stress only depends on the water content. It means that the single soaking conditions only play a role on the capacity of the material to accept more or less water, the yield stress being a direct consequence of the water content.

We then selected experiments corresponding to the same soaking duration of 34 days, and focus on the specific role of each salt. Initial concentrations and ionic strengths are displayed in table 2. The results after soaking are represented by triangles in Fig.7. All the points fall on the master curve (Eq.1), as already pointed out but, more interestingly, a trend can be noticed. The less cohesive state corresponds to the sample soaked in DI water (yield stress falling from 3400 Pa before soaking to 130 Pa after). Then comes the $CaCO_3$ saturated solution followed by NaCl, KCl, $MgCl_2$ and $CaCl_2$ solutions, respectively. We observe that the swelling increases whereas the yield stress decreases when the ionic strength of the soaking solution decreases, in accordance with the expected reduction of the osmotic repulsive forces. Note that ion-ion correlation forces (always attractive) may contribute to the high yield stress (and low swelling) of sediment soaked in solutions of divalent cation salts ($MgCl_2$ and $CaCl_2$). However, the key point in this set of experiments is the sediment strengthening by all the tested salts compared to DI water.

	Salt mass concentration (g/L)	Salt molar concentration (mM)	Ionic strengh (mM)
DI water	~ 0	~ 0	~ 0
$CaCO_3$	0.052	0.52	1.6
NaCl	1.6	27	27
KCl	2.0	27	27
$CaCl_2$	3.0	27	81
$MgCl_2$	2.5	27	81

Table 2 Initial composition, concentration and ionic strength of the soaking solutions used for the experiments presented in Fig. 7. All the solutions have been equilibrated with a gas flow at pCO_2=0.035% (the $CaCO_3$ solution is saturated).

3.2.2 Double soaking. In this set of experiments, the sediment was exposed to two successive soakings. A first soaking was done under the same conditions as in that of section 3.2.1, using DI water or saline solutions. The liquid of this first soaking was removed after 34 days, and replaced by the same volume of DI water, previously equilibrated with an air flow at pCO_2=0.035%. After 24 hours, the sample was removed and its yield stress

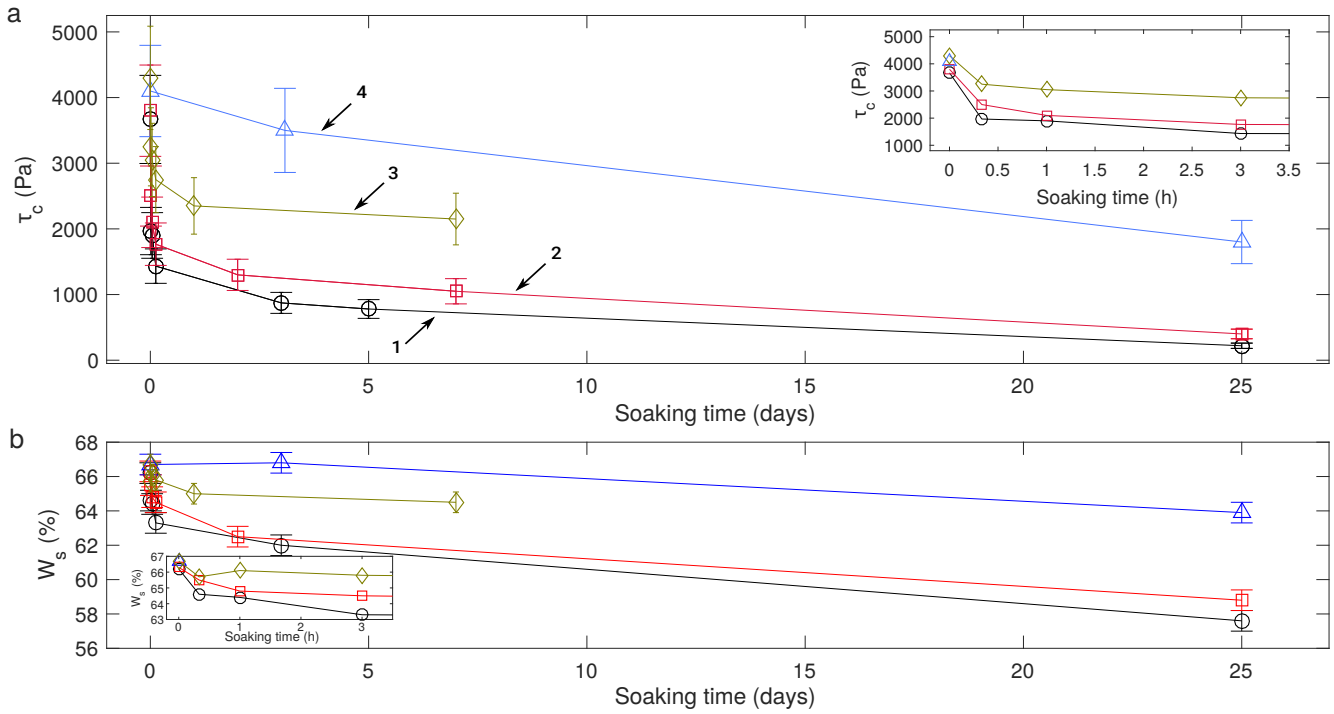

Fig. 6 Time evolution of sediment yield stress τ_c (a) and solid mass fraction W_s (b) in soaking solutions with different concentrations of calcium salts. Each dot represents one soaking experiment. 1) DI water at pCO_2=0.035%; 2) Saturated calcium carbonate solution at pCO_2=0.035% (theoretical solubility is 0.52 mM); 3) Saturated calcium carbonate solution at pCO_2=10% (theoretical solubility is 3.4 mM), 4) $CaCl_2$ concentrated solution (18 mM) at pCO_2=0.035%. For all experiments: sample initial solid fraction is 66.5 ± 0.5% and soaking solution volume is 20 cm^3. A zoom on the first 3 hours is shown in the insets.

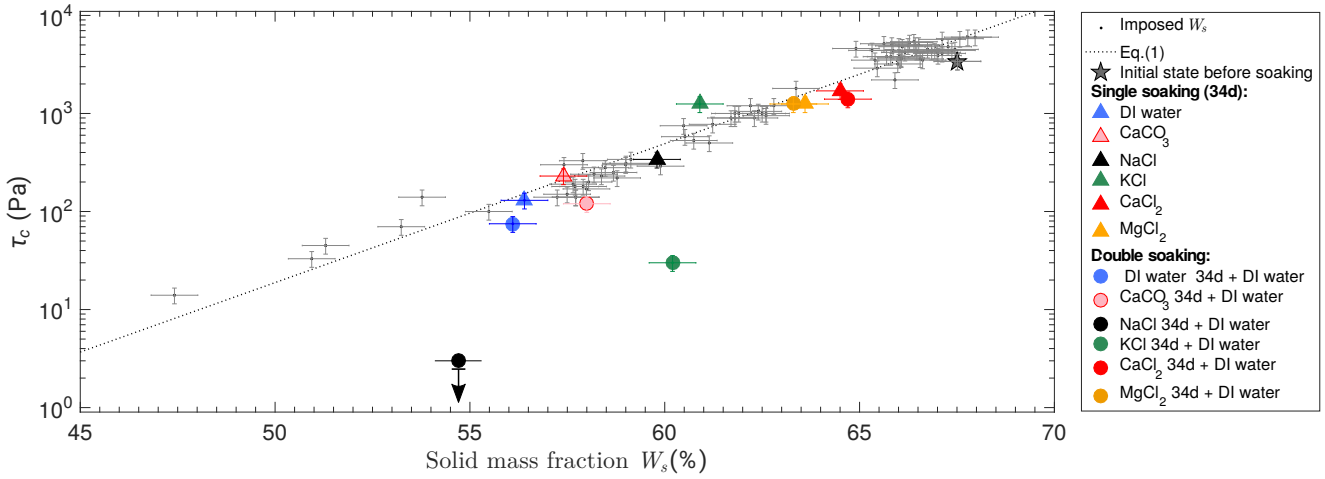

Fig. 7 Sediments yield stress τ_c as a function of the solid mass fraction W_s after single soaking (triangles), double soaking (circles), or for prescribed solid mass fraction (black dots). pCO_2=0.035%, solution volume is 20 cm^3 (the arrow below the black circle means that only a higher bound of the yield stress could be determined).

and solid mass fraction measured. Results are plotted in Fig. 7. Two distinct behaviours are observed.

– When the first soaking was in DI water, $CaCO_3$ saturated solution, $MgCl_2$ solution, or $CaCl_2$ solution, the second soaking in DI water had no significant effect on the solid mass fraction and the yield stress (points after single or double soaking experiments are very close to each other).
– Conversely, after a first soaking in NaCl or KCl solutions, a second soaking in DI water induced a dramatic drop of the yield stress, along with a moderate decrease of the solid mass fraction. Therefore, the corresponding points are strikingly below the master curve. Note that in the case of first soaking in NaCl

solution, a strong turbidity of the second soaking liquid (initially DI water) was observed.

In this case, the yield stress dropped by at least two orders of magnitude during the second soaking in DI water (from 340 Pa to a value smaller than 3 Pa). In this final state, only a higher bound of the yield stress could be determined, and it is even not clear that the sediment is still a yield stress fluid. The corresponding point in Fig. 7 is rejected at least an order of magnitude below the master curve, which means that the yield stress drop cannot be explained by the sample swelling only. With KCl, the effect is still strong, but less pronounced (the yield stress drops by more than an order of magnitude, from 1250 to 30 Pa, and is located an order of magnitude below the master curve). A drastic decrease of the yield stress can thus be obtained by a first soaking in a solution containing a monovalent cation, followed by a second soaking in low-mineralized water.

The phase diagram of Na-smectites (i.e. smectites with Na^+ counterions) has been extensively studied [Abend and Lagaly, 2000, Michot et al., 2004, Bailey et al., 2015, Hedström et al., 2016]. It is well-known that Na-smectites spontaneously disperse when immersed in DI water [Birgersson et al., 2009, Hedström et al., 2016]. Indeed, to prevent particle dispersion by thermal motion, the smectite platelets must form a stiff enough gel. This is the case for: (1) smectites with multivalent counterions, likely because of ion-ion correlations and (2) smectites with monovalent counterions, when the salt concentration is larger than a certain value, the critical coagulation concentration (CCC). Gel phase formation in smectites is generally attributed to the electrostatic interactions between particle faces (negatively charged) and edges (positively charged). When dominant, these attractive interparticle forces prevent particle dispersion. However, with monovalent counterions, at low ionic strength, there is a spillover of the negative potential of faces over the positive edges, which inhibits the formation of edge-to-face bonds [Secor and Radke, 1985, Hedström et al., 2016] and results in particle dispersion.

At this stage, our findings support a predominant role of smectites in the sediment cohesion. The rheological behaviour of our cave sediment can be that this material is made of particles of various compositions and sizes (see section 2.1) binded by smectite, which maintains its cohesion. When the sediment was collected, the dominant counterion in smectite was certainly calcium (Ca^{2+}), as it is the most common cation in a karstic environment. Furthermore, divalent Ca^{2+} counterions prevent dispersion of smectite particles when the sediment is immersed in DI water. This holds true for a sediment sample after a first soaking in $CaCl_2$ or $MgCl_2$ solutions, which can only strengthen the material by increasing the proportion of divalent cations in the counterion layer. After a first soaking in a solution of NaCl or KCl, monovalent cations Na^+ or K^+ are substituted for Ca^{2+} counterions. No dramatic collapse of the yield stress is observed at this stage because the ionic strength of this first soaking solution is larger than the CCC and Na-smectite remains in a gel state. This is no longer the case after immersion in DI water. Smectite – colloidal – particles are dispersed by thermal motion (as evidenced by the increase of solution turbidity), the yield stress of the sediment dramatically drops because it looses its binder, and a small mechanical stress can be sufficient to induce sediment migration.

This suggests that a vermiculation crisis could be explained by a two-step scenario. Most of the time, the dominant cation in water films lying on cave walls is Ca^{2+}, which results in strong cohesion of the sediment layer. A first step would consist in a change of physico-chemical conditions (due for instance to evaporation or biological activity) leading to predominance of monovalent ions in the liquid layer. Notice that, assuming $[Ca^{2+}] \sim 1\,\text{mM}$, a transition from Ca-smectite to Na-smectite behaviour requires at least $[Na^+] \sim 10\,\text{mM}$ (derived from Eq.2.1 and data in [Birgersson et al., 2011]). Such a monovalent cation concentration is likely to result in a ionic strength above the smectite CCC, with no drastic reduction of sediment cohesion. However, the sediment yield stress will surely collapse if, in a second step, a condensation event occurs before returning to a Ca^{2+} dominant situation.

Interestingly enough, the mechanism described above is known to act in very different situations. Quick clay is an unstable soil susceptible of serious landslides. Na^+ is the most abundant cation in these marine sediments. It has been shown that the risk of landslide is negatively correlated with water salinity [Andersson-Sköld et al., 2005]. Therefore, rainfall is a common cause of quick clay landslides, because the leaching of salts gives rise to an increase in the double layer repulsion and a loss of cohesion of the material [Rosenqvist, 1966]. Another interesting situation, showing strong similarities with our experiments, is erosion of bentonite buffers used for nuclear waste repositories (bentonite consists mainly of montmorillonite, a smectite clay). It has been shown in laboratory experiments [Birgersson et al., 2009, Hedström et al., 2016] that erosion was related to the gel-sol transition occurring with Na-smectite in low-mineralized water. No erosion was observed with Ca-smectite, or Na-smectite above a certain ionic strength.

Changes in hydrochemical conditions could also possibly play a role in variations of turbidity observed at karst springs. Conditions leading to a drop of yield stress of Na-smectites are potentially encountered in soils, especially in the upper part. This might be a strong parameter controlling particle input into karst systems, and correspondingly turbidity of karst springs.

4 Conclusion

Vermiculations have been recently reported in valuable painted caves, where they are a potential cause of damages, since they result in displacement of the material (including pigments) initially at rest on the walls. It turns out that the policies of conservation of these caves must be improved, which requires the understanding of the physical mechanisms at play. For this purpose, we have carried out laboratory experiments to identify conditions which can cause a yield stress decrease of the cave sediment, and enable sediment migration and vermiculation formation. Sediments have been collected in different karstic caves in Dordogne, including Lascaux. As the sediments were very similar, in composition and particle distribution, we have focused our study on sediment from Maillol cave, which may likely be considered as a model material for other caves in Dordogne. The sediment exhibits a yield stress, ranging from 6000 Pa to 14 Pa for a solid volume fraction ranging from approximately 45% to 25%. This yield stress can be attributed to the presence of colloidal particles, mainly composed of smectite clay. We have identified two different scenarios of yield stress decrease which could trigger or facilitate a vermiculation crisis.

- When soaked in low-mineralized water, the sediment yield stress exhibits a rapid and limited drop, followed by a slow decrease, which can seriously weaken the sediment layer if soaking is continued over several months. A long condensation period in a cave environment is thus a favourable condition for particle migration on a cave wall (and a dangerous situation for caves paintings).
- A much more spectacular drop of sediment yield stress (up to 2 orders of magnitude in 24 hours) is observed when the sediment is successively soaked into a solution containing monovalent cations and in low-mineralized water. If a similar scenario occurs in a cave, sediment will certainly be able to migrate, resulting in painting degradation.

We interpret the first step of this second scenario as the substitution of monovalent ions to Ca^{2+} in the diffuse layer of smectite platelets. This process requires a monovalent ion activity far exceeding the calcium one. How such conditions can be reached in natural karstic environment have still to be addressed and elucidated. For example the complexation of calcium by organic molecules such as humic acids or alginates can decrease the activity of calcium ions. Microbiological activity is known to change the physicochemical environment, and is certainly a promising line of investigation.

Acknowledgments

This study is part of investigations supported by the French Ministry of Culture, Direction des Affaires Culturelles de Nouvelle-Aquitaine. We want to thank them and their sub-contractants for support and data. In this context we want to thank more specifically Jean-Christophe Portais and Sandrine Géraud for their help. We gratefully thank A. Aubertin, L. Auffray, J. Amarni, R. Pidoux and C. Manquest (FAST Laboratory) for technical support. We thank D. Calmels, C. Quantin, G. Monvoisin, O. Dufaure and S. Miska (GEOPS Laboratory) for chemical analysis and geological characterization of our samples. We thank P. Coussot and A. Fall (from Laboratoire Navier), B. Cabane (from LCMD) and J.B. Salmon (from LOF) for useful discussions.

References

[Abend and Lagaly, 2000] Abend, S. and Lagaly, G. (2000). Sol-gel transitions of sodium montmorillonite dispersions. *Applied Clay Science*, 16(3):201 – 227.

[Andersson-Sköld et al., 2005] Andersson-Sköld, Y., Torrance, J. K., Lind, B., Odén, K., Stevens, R. L., and Rankka, K. (2005). Quick clay-a case study of chemical perspective in southwest sweden. *Engineering Geology*, 82(2):107 – 118.

[Anger, 2011] Anger, R. (2011). *Approche granulaire et colloïdale du matériau terre pour la construction*. PhD thesis, Institut National des Sciences Appliquées de Lyon.

[Aran et al., 2008] Aran, D., Maul, A., and Masfaraud, J. (2008). Surface geosciences (pedology). *Comptes rendus - Geoscience*, 340(12):865–871.

[Bailey et al., 2015] Bailey, L., Lekkerkerker, H. N. W., and Maitland, G. C. (2015). Smectite clay - inorganic nanoparticle mixed suspensions: phase behaviour and rheology. *Soft Matter*, 11:222–236.

[Barr, 1957] Barr, T. C. (1957). A possible origin for cave vermiculations. *National Spelological Society News*, 16(3):34–35.

[Barton and Northup, 2007] Barton, H.-A. and Northup, D.-E. (2007). Geomicrobiology in cave environments: Past, current and future perspectives. *Journal of Cave and Karst Studies*, 69(1):163 – 178.

[Bini, 1975] Bini, A. (1975). Le "vermiculazioni argillose" de la grotta zelbio (2037 loco). *Il Grottesco*, 36:5–14.

[Bini et al., 1978] Bini, A., Cavalli Gori, M., and S., G. (1978). A critical review of hypotheses on the origin of vermiculations. *Int. J. Speleol.*, 10:11–33.

[Birgersson et al., 2009] Birgersson, M., Börgesson, L., Hedström, M., Karnland, O., and Nilsson, U. (2009). Bentonite erosion. Final report. Technical Report TR-09-34, SKB.

[Birgersson et al., 2011] Birgersson, M., Hedström, M., and Karnland, O. (2011). Sol formation ability of Ca/Na-montmorillonite at low ionic strength. *Physics and Chemistry of the Earth, Parts A/B/C*, 36(17):1572 – 1579. Clays in Natural & Engineered Barriers for Radioactive Waste Confinement.

[Carrière et al., 2018] Carrière, S. R., Jongmans, D., Chambon, G., Bièvre, G., Lanson, B., Bertello, L., Berti, M., Jaboyedoff, M., Malet, J.-P., and Chambers, J. E. (2018). Rheological properties of clayey soils originating from flow-like landslides. *Landslides*, 15(8):1615–1630.

[Clottes, 1981] Clottes, J. (1981). Midi-Pyrénées. *Gallia Préhistoire*, 24(2):525–570.

[Coussot and Ancey, 1999] Coussot, P. and Ancey, C. (1999). Rheophysical classification of concentrated suspensions and granular pastes. *Phys. Rev. E*, 59:4445–4457.

[Coussot et al., 2002] Coussot, P., Nguyen, Q. D., Huynh, H. T., and Bonn, D. (2002). Avalanche behavior in yield stress fluids. *Phys. Rev. Lett.*, 88:175501.

[Faucher and Lauriol, 2016] Faucher, B. and Lauriol, B. (2016). Les vermiculations de la grotte Wilson (Lac la Pêche, Québec, Canada). Contexte morphoclimatique, analyses sédimentologiques et distribution spatiale. *Géomorphologie: relief, processus, environnement*, 22:96–103.

[Ford and Williams, 2007] Ford, D. C. and Williams, P. W. (2007). *Karst Hydrogeology and Geomorphology*. Wiley & Sons.

[Gaillardet et al., 2018] Gaillardet, J., Calmels, D., Romero-Mujalli, G., Zakharova, E., and Hartmann, J. (2018). Global climate control on carbonate weathering intensity. *Chemical Geology*, In Press.

[Hedström et al., 2016] Hedström, M., Hansen, E.-E., and Nilsson, U. (2016). Montmorillonite phase behaviour. Relevance for buffer erosion in dilute groundwater. Technical Report TR-15-07, SKB.

[Hoerlé, 2012] Hoerlé, S. (2012). État des connaissances et étude minérale des vermiculations de la grotte de Lascaux. Volet 1 - État des connaissances sur les vermiculations. *Reports on "Vermiculations in Lascaux cave", French Ministry of Culture*.

[Hœrlé et al., 2011] Hœrlé, S., Konik, S., and Chalmin, É. (2011). Les vermiculations de la grotte de Lascaux : identification de sources de matériaux mobilisables par microanalyses physico-chimiques. *Karstologia*, 58(1):29–40.

[Jönsson et al., 2009] Jönsson, B., Åkesson, T., Jönsson, B., Meehdi, S., Janiak, J., and Wallenberg, R. (2009). Structure and forces in bentonite MX-80. Technical Report TR-09-06, SKB.

[Khaldoun et al., 2009] Khaldoun, A., Moller, P., Fall, A., Wegdam, G., De Leeuw, B., Méheust, Y., Otto Fossum, J., and Bonn, D. (2009). Quick clay and landslides of clayey soils. *Phys. Rev. Lett.*, 103:188301.

[Konik et al., 2014] Konik, S., Lafon-Pham, D., Riss, J., Aujoulat, N., Ferrier, C., Kervazo, B., Plassard, F., and Reiche, I. (2014). Étude des vermiculations par caractérisations morphologique, chromatique et chimique. L'exemple des grottes de Rouffignac et de Font-de-Gaume (Dordogne, France). *Paleo*, Special Issue:311 – 321.

[Larson, 1999] Larson, R. G. (1999). *The structure and rheology of complex fluids*. Oxford University Press.

[Magnin and Piau, 1987] Magnin, A. and Piau, J. (1987). Shear rheometry of fluids with a yield stress. *Journal of Non-Newtonian Fluid Mechanics*, 23:91 – 106.

[Magnin and Piau, 1990] Magnin, A. and Piau, J. (1990). Cone-and-plate rheometry of yield stress fluids. Study of an aqueous gel. *Journal of Non-Newtonian Fluid Mechanics*, 36:85 – 108.

[Martel, 1906] Martel, E. A. (1906). Étude de la source de Fontaine-L'Évêque (Var). *Annales d'Hydraulique Agricole*, 34:374–381.

[Martin et al., 2006] Martin, C., Pignon, F., Magnin, A., Meireles, M., Lelièvre, V., Lindner, P., and Cabane, B. (2006). Osmotic compression and expansion of highly ordered clay dispersions. *Langmuir*, 22(9):4065–4075. PMID: 16618146.

[Martin et al., 2002] Martin, C., Pignon, F., Piau, J.-M., Magnin, A., Lindner, P., and Cabane, B. (2002). Dissociation of thixotropic clay gels. *Phys. Rev. E*, 66:021401.

[Michot et al., 2004] Michot, L., Bihannic, I., Porsch, K., Maddi, S., Baravian, C., Mougel, J., and Levitz, P. (2004). Phase diagrams of Wyoming Na-montmorillonite clay. Influence of particle anisotropy. *Langmuir*, 25(20):10829–10837.

[Norrish, 1954] Norrish, K. (1954). The swelling of montmorillonite. *Discussions of the Faraday Society*, 18:120–134.

[Ovarlez et al., 2015] Ovarlez, G., Mahaut, F., Deboeuf, S., Lenoir, N., Hormozi, S., and Chateau, X. (2015). Flows of suspensions of particles in yield stress fluids. *J. Rheol.*, 59:1449–1486.

[Plummer and Wigley, 1976] Plummer, L.-N. and Wigley, T.-M.-L. (1976). The dissolution of calcite in CO_2-saturated solutions at 25°C and 1 atmosphere total pressure. *Geochimica et Cosmochimica Acta*, 40(2):191 – 202.

[Reddy et al., 1990] Reddy, K., Lindsay, W., Workman, S., and Drever, J. (1990). Measurement of calcite ion activity products in soils. *Soil Sci. Soc. Am. J.*, 54:67–71.

[Rosenqvist, 1966] Rosenqvist, I. (1966). Norwegian research into the properties of quick clay-a review. *Engineering Geology*, 1(6):445 – 450.

[Secor and Radke, 1985] Secor, R. and Radke, C. (1985). Spillover of the diffuse double layer on montmorillonite particles. *Journal of Colloid and Interface Science*, 103(1):237 – 244.

[Segad et al., 2010] Segad, M., Jönsson, B., Åkesson, T., and Cabane, B. (2010). Ca/Na montmorillonite: Structure, forces and swelling properties. *Langmuir*, 26(8):5782–5790. PMID: 20235552.

[White, 2015] White, W. (2015). Chemistry and karst. *Acta Carsologica*, 44(3):349 – 362.